

NONEQUILIBRIUM EFFECTS IN CHEMICAL WAVE
FRONTS: MICROSCOPIC SIMULATIONS AND
ANALYTICAL APPROACH*

ANNIE LEMARCHAND

Université Pierre et Marie Curie
Laboratoire de Physique Théorique des Liquides, C.N.R.S. U.R.A. 765
4, place Jussieu, 75252 Paris Cedex 05, France

B. NOWAKOWSKI

Institute of Physical Chemistry, Polish Academy of Sciences
Kasprzaka 44/52, 01-224 Warsaw, Poland
Warsaw Agricultural University
Rakowiecka 28, 02-528 Warsaw, Poland

M.A. KARAZI

Université Pierre et Marie Curie
Laboratoire de Physique Théorique des Liquides, C.N.R.S. U.R.A. 765
4, place Jussieu, 75252 Paris Cedex 05, France

(Received November 28, 1997)

Using a Monte Carlo simulation to generate a reaction-diffusion wave front, we find that its mean propagation speed and profile width are smaller than their macroscopic predictions. These discrepancies are related to departures from equilibrium particle velocity distribution for fast reactions. To improve the prediction of macroscopic front properties, we deduce from Boltzmann equation the corrections to the macroscopic equation governing the evolution of chemical species concentrations.

PACS numbers: 82.20. -w, 05.70. Ln, 47.70. Fw

* Presented at the Marian Smoluchowski Symposium on Statistical Physics, Zakopane, Poland, September 1-10, 1997.

1. Introduction

A microscopic simulation of Monte Carlo type is used to generate a chemical wave front propagating in a one-dimensional (1D) medium. This paper intends to bring out the microscopic phenomena which control the macroscopic dynamics and to present how the macroscopic description must be supplemented to correctly predict the wave-front behavior. The chemical model chosen, introduced by Fisher [1] and Kolmogorov *et al.* [2], involves two species A and B which diffuse with an identical coefficient D and react according to



If the total concentration of species A and B,

$$n_C = n_A(x, t) + n_B(x, t) \quad (2)$$

is initially homogeneous, n_C remains constant whatever position x and time t . The macroscopic deterministic evolution of the local fraction $A(x, t) = n_A/n_C$ of particles A obeys the following equation [1,2]

$$\partial_t A = kA(1 - A) + D\partial_x^2 A, \quad (3)$$

where k is a rate constant. Equation (3) admits a family of wave-front solutions $A(x, t) = a(\zeta)$, where $\zeta = x - Ut$, moving with a constant speed U and replacing the unstable $A \equiv 0$ stationary state by the stable $A \equiv 1$ stationary state. The macroscopic dynamics (3) only imposes a lower bound

$$U_{\min} = 2\sqrt{kD} \quad (4)$$

on the continuous range of velocities U associated with linearly stable fronts. According to the so-called marginal stability criterion [3], a large class of sufficiently steep initial profiles evolves to the front associated with U_{\min} . A workable definition of the profile width E_{\min} is provided by the inverse of the steepness at the inflexion point and an expansion [4] of Eq. (3) in $1/U_{\min}^2$ leads to the estimate value:

$$E_{\min} \simeq 8\sqrt{D/k}. \quad (5)$$

Our aim is to discuss the ability of the macroscopic theory to predict the mean properties of a wave front generated within a microscopic modelization of the system. Deviations from macroscopic predictions (4) and (5) in molecular dynamics simulations of dense fluids have been observed and interpreted [5] in terms of extended irreversible thermodynamics [6]. On the

other hand, it is well-known [7] that a chemical reaction may induce perturbations of the particle velocity distribution. At a macroscopic description level, an important consequence of this deformation is the modification of reaction rate constants and transport coefficients [8]. The Direct Simulation Monte Carlo (DSMC) method introduced by Bird [9] will allow us to test possible nonequilibrium effects on a macroscopic pattern like a wave front.

2. Microscopic simulation method

Following Bird [9], we consider a dilute gas of hard spheres. The medium is divided into linearly arranged cells of length Δl equal to a fraction of the mean free path. During the simulation time step Δt chosen as a fraction of the mean free time, the free motion of particles and their mutual collisions are supposed to be uncoupled. The particle motion is simulated in 1D. The section of the cells is chosen so as to ensure dilute conditions. The collisions are performed in 3D as follows. A collision between a pair (i, j) of particles, randomly chosen in a same cell, is accepted if their relative speed obeys:

$$|\mathbf{v}_i - \mathbf{v}_j| > Rv_{\max}^r, \quad (6)$$

where $0 \leq R \leq 1$ is a random number and v_{\max}^r is a continuously updated maximum relative speed. The postcollision velocities are deduced from the energy and impulsion conservation laws for a random impact parameter. A cell time variable is increased by an evaluation of the colliding pair approach time and new collisions are performed until the cell time reaches Δt . Reaction (1) is supposed to have a vanishing activation energy but only occurs with a given probability s_f which plays the role of a steric factor. More precisely, an accepted collision between different species is reactive if

$$s_f > R', \quad (7)$$

where $0 \leq R' \leq 1$ is a random number.

This procedure is repeated in each cell at each time step. In appropriate conditions discussed further (small s_f), we verify that the simulated values of rate constant k and diffusion coefficient D coincide with their equilibrium predictions according to Boltzmann formulation [9]

$$\begin{aligned} k &= 4n_C d^2 \sqrt{\frac{\pi k_B T}{m}} s_f \\ D &= \frac{3}{8} \frac{1.017}{n_C d^2} \sqrt{\frac{k_B T}{\pi m}}, \end{aligned} \quad (8)$$

where d and m are respectively the diameter and mass of the hard spheres considered, k_B is the Boltzmann constant, and T denotes the temperature.

3. Simulation results

We choose specific boundary conditions in order to mimic the propagation of a front of particles A in an infinite medium. Initially, particles A are located in the left cells, particles B in the right cells. When the total number of particles A becomes greater than its initial value, the first left cell becomes the last right one while its particles A are transformed into B's and the front position $\phi(t)$ is increased by Δl . For the parameter values chosen, this trick is actually performed only every 100 or 1000 time steps on average. It amounts to switch into a frame moving with speed $U(t)$, equal to the time derivative of $\phi(t)$, hence appearing as the now fluctuating front speed. Independently of the microscopic realization of the initial condition, the time average $\langle a(\zeta) \rangle$ of the local fraction of particles A in cell ζ of the moving frame evolves to a stationary profile as depicted on Fig. 1. In the following, $\langle \rangle$ refers to a time average over the simulation time after the stationary regime has been reached.

For a vanishing activation energy and a steric factor $s_f = \exp(-0.5)$, the mean profile width $\langle E \rangle$ and the mean front propagation speed $\langle U \rangle$ are both about 15% smaller than their deterministic predictions given by Eqs (4), (5). As shown on Fig. 2, these deviations from the deterministic theory monotonically regress as s_f varies from 1 to 0 but are still perceptible for $s_f = \exp(-7)$. Intuitively, the faster the reaction, the less efficient the thermalization between two close reactive collisions.

In order to quantify the effect of the chemical reaction on the velocity distribution of particles A without taking into account the inhomogeneities in the front propagation direction x , we determine the second moment $\langle v_y^2 + v_z^2 \rangle$ of the distribution restricted to coordinates y and z . As shown in Fig. 1 for $s_f = \exp(-0.5)$, the second moment $\langle v_y^2 + v_z^2 \rangle$ of particle A velocity distribution, considered as a function of space variable ζ in the moving frame, presents around the front position a clear increase with respect to its equilibrium value $2k_B T/m$. Whatever the steric factor, the relative deviation

$$\frac{\Delta \langle v_y^2 + v_z^2 \rangle}{\langle v_y^2 + v_z^2 \rangle_{\text{eq}}} = \frac{\langle v_y^2 + v_z^2 \rangle - 2k_B T/m}{2k_B T/m}$$

tends to a limit in the leading edge of the front. The perturbation suddenly disappears on the right when the fraction $\langle a(\zeta) \rangle$ of particles A vanishes. Note that obtaining Fig. 1, *i.e.* one point on Fig. 2, requires weeks of computation on an up-to-date workstation, and that CPU time increases with $-\ln(s_f)$. In spite of the very large number of simulation time steps considered to compute

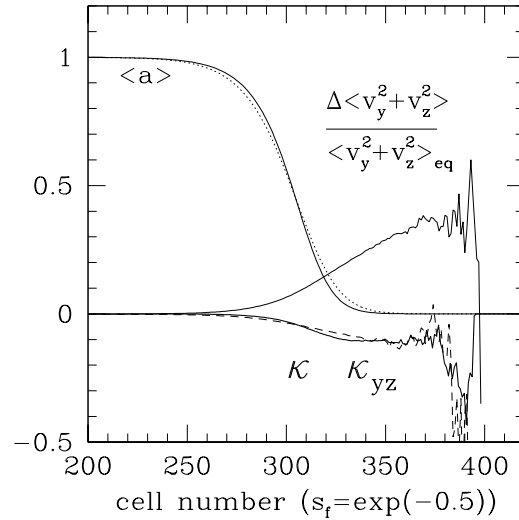


Fig. 1. Simulation results: spatial variations in the moving frame of the isotropic kurtosis κ (solid line) and the nonisotropic kurtosis κ_{yz} (long-dashed line) of the A particle velocity distribution, of the relative deviation of its second moment $\langle v_y^2 + v_z^2 \rangle$ to its equilibrium value $2k_B T/m$ and comparison of time averaged fraction $\langle a(\zeta) \rangle$ of particles A (solid line) with the corresponding profile predicted by the macroscopic deterministic theory (short-dashed line). The simulation parameters take the following values: steric factor $s_f = \exp(-0.5)$, density $n_C = 0.1$, temperature $k_B T = 1$, mass $m = 1$, diameter $d = 1$. The average is performed over a time corresponding to more than 2×10^8 reactive collisions.

$\frac{\Delta \langle v_y^2 + v_z^2 \rangle}{\langle v_y^2 + v_z^2 \rangle_{\text{eq}}}$, oscillations around the limit in the leading edge are observed because of the very small number of particles A in the most advanced part of the front.

The effect of the chemical reaction (1) does not only consist of an increase of the effective temperature associated with particles A (and jointly of a cooling of B's, since the total kinetic energy is constant) but also of a deviation from the Gaussian character of the particle velocity distribution. This departure from the Maxwellian statistics is quantified by non vanishing values of the kurtosis restricted to coordinates y and z

$$\kappa_{yz} = \left(\frac{m}{2k_B T} \right)^2 (\langle (v_y^2 + v_z^2)^2 \rangle - 2\langle v_y^2 + v_z^2 \rangle^2) \quad (9)$$

around the front zone. Note that the spatial variations in the moving frame

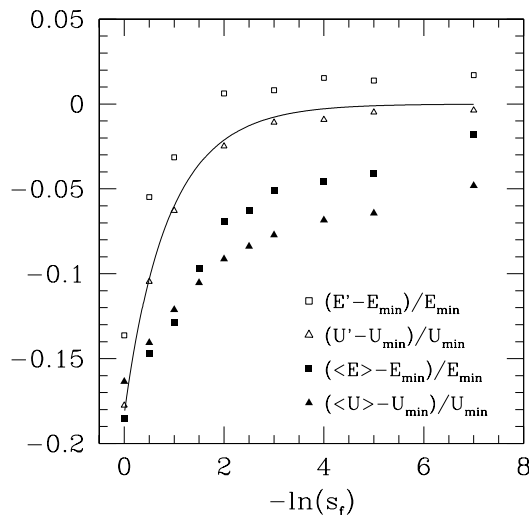


Fig. 2. Comparison between simulation results (solid symbols) and the analytical approach based on the Boltzmann equation (open symbols): relative deviations from their macroscopic prediction of the time averaged profile width (square) and front propagation speed (triangle) as functions of $-\ln(s_f)$, where s_f is the steric factor. The solid line gives the values calculated from Eqs (19), (20).

of the isotropic kurtosis defined as

$$\kappa = \left(\frac{m}{3k_B T} \right)^2 \left(\langle v^4 \rangle - \frac{5}{3} \langle v^2 \rangle^2 \right) \quad (10)$$

nearly coincide with the variations of κ_{yz} as shown on Fig. 1. The non vanishing values of κ or κ_{yz} in the leading edge of the front proves that the chemical system does not relax toward the equilibrium distribution between two successive reactive collisions: the standard hypothesis of local equilibrium is not valid in a medium traveled by a chemical wave front even for relatively slow reactions. Deviations are still observable for a steric factor obeying $-\ln(s_f) = 7$.

The relation between the change in mean wave-front properties and the non Maxwellian character of the distribution is supported by the decay of both effects as the steric factor decreases and the reaction becomes slower. As early observed in homogeneous conditions [7] and confirmed for inhomogeneous systems [8], choosing a reactive criterion independent of the relative energy of the colliding pair does not prevent from observing nonequilibrium effects. For the chemical wave front studied here, reaction (1) may occur only between particles A and B obeying collision criterion (6). To mimic Boltzmann collision term, the selection of a pair of colliding particles de-

pends on their relative speed. Therefore, the change of nature of a particle B into a particle A does not affect equally the entire population of particles B so that reaction (1) induces deviations from Maxwellian distribution for each chemical species even in the case of the stochastic rule (7) adopted here to accept a reactive collision.

4. Analytical approach

In order to interpret the numerical results in the framework of kinetic theory, we consider the Boltzmann equations for the distribution functions $f_A(x, \mathbf{v}, t)$ and $f_B(x, \mathbf{v}, t)$ of species A and B, respectively. The isothermal reaction (1) which only changes the chemical identity of molecules does not affect the velocity distribution of the mixture as a whole. Consequently, the initial equilibrium of the whole system is maintained all the time. It means that

$$f_A + f_B = n_C \exp\left(-\frac{mv^2}{2k_B T}\right), \quad (11)$$

where the uniform total concentration n_C is defined in Eq. (2). The Boltzmann equation for A can be written as

$$\begin{aligned} \partial_t f_A + v_x \partial_x f_A &= \int (f'_A f'_{A1} - f_A f_{A1}) |\mathbf{v} - \mathbf{v}_1| d\sigma_{AA} d\mathbf{v}_1 \\ &+ \int (f'_A f'_B - f_A f_B) |\mathbf{v} - \mathbf{v}_B| d\sigma_{AB} d\mathbf{v}_B \\ &+ \int f'_A f'_B |\mathbf{v} - \mathbf{v}_B| d\sigma_{AB}^* d\mathbf{v}_B, \end{aligned} \quad (12)$$

where σ_{AA} and σ_{AB} are the cross sections for elastic collisions of hard spheres A–A and A–B, respectively, and σ_{AB}^* is the cross section for reaction (1). The reaction rate constant and the diffusion coefficient can be calculated from the Boltzmann equation by means of the Chapman-Enskog method [10]. This perturbative approach was applied to homogeneous reactive systems previously [7]. We use here an extension of this method assuming that the chemical process as well as the transport process can be treated as a perturbation. Equation (11) is used to eliminate f_B in the Boltzmann equation (12) for the distribution function of A. Moreover, Eq. (11) implies the following relation between the temperatures $T_A(x, t)$ and $T_B(x, t)$ specific to each species A and B:

$$n_A(x, t)T_A(x, t) + n_B(x, t)T_B(x, t) = n_C T. \quad (13)$$

The deformation of the velocity distribution induced by the chemical reaction leads in the third order approximation to modified expressions k' and D' for the rate coefficients depending now on the local fraction $A(x, t)$ as:

$$k' = k(\alpha_0 + \alpha_1 A(x, t)) , \quad (14)$$

$$D' = D(\beta_0 + \beta_1 A(x, t)) , \quad (15)$$

with

$$\alpha_0 = 1 + \frac{43}{640} s_f, \quad \alpha_1 = -2(\alpha_0 - 1), \quad (16)$$

$$\beta_0 = 1 - \frac{7583}{20532} s_f, \quad \beta_1 = -2(\beta_0 - 1). \quad (17)$$

The above equations state that the correction to the diffusion coefficient is larger than that to the rate constant.

Moreover the solution of Eq. (12) yields at this level of approximation a quadratic term proportional to $(\partial_x A)^2$, so that the macroscopic equation is now given by:

$$\partial_t A = k' A(1 - A) + D' \partial_x^2 A + q(\partial_x A)^2 , \quad (18)$$

with $q = (D/24) s_f$. The above equation does not have the form of the simple reaction-diffusion equation (3) and the formulas (4,5) for speed and width of the front cannot be applied directly. We first numerically integrate Eq. (18) with the same steep initial condition as in the simulation. Whatever the steric factor, we obtain a stationary front profile in a frame moving at a constant speed. The variations with the steric factor of the profile width E' and propagation speed U' deduced from the numerical integration of Eq. (18) are represented in Fig. 2. Secondly, we perform a linear stability analysis of Eq. (18) in the leading edge of the front where $A(x, t)$ vanishes. The minimum speed predicted in the frame of the marginal stability criterion [3] obeys:

$$U'_{\min} = U_{\min} \sqrt{\alpha_0 \beta_0} . \quad (19)$$

Expanding Eq. (18) in power of $1/(U'_{\min})^2$ leads [4] to an approximate value of the width E'_{\min} of the front propagating at U'_{\min} :

$$E'_{\min} = E_{\min} \sqrt{\alpha_0 \beta_0} \left(1 + \frac{s_f}{384 \alpha_0 \beta_0} \right)^{-1} . \quad (20)$$

The relative corrections of speed and width to their macroscopic predictions U_{\min} and E_{\min} practically coincide.

5. Conclusion

The results of the different approaches may be compared in Fig. 2. The analytical approach based on the Boltzmann equation and the simulation results predict both a slowing down of the front and an enhancement of its steepness with respect to the macroscopic description. These observable deviations from the macroscopic predictions are related to departures from the equilibrium particle velocity distribution. It is worth to note that the negative correction to the diffusion coefficient is essential to explain the decrease of the speed. The prediction of speed by the marginal stability analysis agrees very well with the result deduced from the numerical integration of Eq. (18). For the width, a small difference between these results can be noticed. The quantitative agreement between simulation and theory is not entirely satisfactory. For large steric factors close to 1, the differences observed can be attributed to the limitations of the Chapman-Enskog method which is not valid for very fast reactions. Moreover, the standard diffusion equation does not describe completely correctly transport processes in which large inhomogeneities are involved [6], like in a very steep front. However, these effects should be less important for steric factors smaller than $\exp(-3)$ where some differences are still detected.

This work was possible thanks to the support POL/1639 from CNRS (France) and Polish Academy of Sciences.

REFERENCES

- [1] R.A. Fisher, *Ann. Eugenics* **7**, 335 (1937).
- [2] A. Kolmogorov, I. Petrovsky, N. Piskunov, *Bull. Univ. Moscow. Ser. Int. Sec. A* **1**, 1 (1937).
- [3] D.G. Aronson, H.F. Weinberger, *Adv. Math.* **30**, 33 (1978); W. van Saarloos, *Phys. Rev. Lett.* **58**, 2571 (1987); *Phys. Rev.* **A37**, 211 (1988); **39**, 6367 (1989).
- [4] J.D. Murray, *Mathematical Biology*, Springer, Berlin 1989.
- [5] J. Gorecki, *Physica*, **D84**, 171 (1995).
- [6] B.C. Eu, *Kinetic Theory and Irreversible Thermodynamics* Wiley, New York 1992.
- [7] I. Prigogine, E. Xhrouet, *Physica* **15**, 913 (1949); B. Shizgal, M. Karplus, *J. Chem. Phys.* **52**, 4262 (1970); *J. Chem. Phys.* **54**, 4345 and 4357 (1971); B. Shizgal, D. Napier, *Physica* **A223**, 50 (1996).
- [8] B. Nowakowski, J. Popielawski, *J. Chem. Phys.* **100**, 7602 (1994); B.V. Alexeev, A. Chikhaoui, I.T. Grushin, *Phys. Rev. E* **49**, 2809 (1994); B. Nowakowski, A. Lemarchand, *J. Chem. Phys.* **106**, 3965 (1997).

- [9] G. A. Bird, *Molecular Gas Dynamics and the Direct Simulation of Gas Flows*, Clarendon, Oxford 1994.
- [10] S. Chapman, T.G. Cowling, *The Mathematical Theory of Nonuniform Gases* Cambridge University Press, London 1953.